MRI Brain Image Segmentation Using an AM-FM Model

Marios S. Pattichis[1], Helen Petropoulos[2], and William M. Brooks[2]

[1]Department of Electrical and Computer Engineering, The University of New Mexico, Albuquerque, NM, 87131, e-mail: pattichis@eece.unm.edu

[2]Clinical & Magnetic Resonance Research Center, The University of New Mexico, Albuquerque, NM 87131, e-mail: {eleni, brooks}lizard.unm.edu

Abstract - *MRI brain images are characterized by non-stationary components that make fully automated segmentation a challenging task. An AM-FM model is used to model these non-stationarities. Using the AM-FM model, a new, fully automated texture segmentation system is used to automatically segment the cerebellum from a 3-D set of MRI brain images.*

I. Introduction

The cerebellum segmentation problem is illustrated in Figure 1. Given a collection of manually segmented MRI images, we seek to use an automated algorithm that uses these images to compute a segmentation for a collection of new images. To measure the success of the method, all images were manually-segmented and this allows us to measure the results on the "test" images against the ground-truth.

The automated segmentation algorithm is designed to be: (i) translation-invariant, (ii) rotation-invariant, and also allow for a simple method for adopting the algorithm for (iii) scale-invariance. To model the MRI image, we require the use of a non-stationary model that can provide a natural representation for strong spatial variations in brain structure. In particular, we note the distinct directional variation throughout the cerebellum that clearly distinguishes it from its background. For constant, equal pattern spacing in the cerebellum, we could use a constant period sinusoid for representing the image. However, to account for the observed spatial variations in the pattern periodicity, we use and AM-FM model [1-4]:

$$\begin{aligned} I(\mathbf{x}) \;=\; & a_{cer}(\mathbf{x})\sum_{n,m} A_{n,m} \\ & \exp\left[j2\pi\left(\frac{n}{T_1}\phi_1(\mathbf{x})+\frac{m}{T_2}\phi_2(\mathbf{x})\right)\right] \\ & + a_{non-cer}(\mathbf{x})\sum_{n,m} B_{n,m} \\ & \exp\left[j2\pi\left(\frac{n}{T_1}\psi_1(\mathbf{x})+\frac{m}{T_2}\psi_2(\mathbf{x})\right)\right] \end{aligned} \quad (1)$$

where the first summation describes the image over the cerebellum, while the second summation describes the image over the non-cerebellum regions. We note that at any given pixel, only one of the two amplitude functions is non-zero. If a pixel belongs to the cerebellum, then the cerebellum amplitude is non-zero: $a_{cer}(\mathbf{x})\neq 0$, while the non-cerebellum amplitude is zero: $a_{non-cer}(\mathbf{x})=0$. Conversely, if a pixel is not part of the cerebellum: $a_{cer}(\mathbf{x})=0$, $a_{non-cer}(\mathbf{x})\neq 0$. Using (1), an arbitrary MRI image can be described in terms of the amplitude functions: $a_{cer}, a_{non-cer}$, the phase functions: $\phi_1,\phi_2,\psi_1,\psi_2$ and the AM-FM series coefficients: $A_{n,m}, B_{n,m}$. To segment the image into cerebellum versus non-cerebellum regions, we will only use: $a_{cer}, a_{non-cer}$. To estimate these functions, we use Dominant Component Analysis (DCA) [1-4].

The amplitude functions were found to maintain distinct values when describing cerebellum structure, as opposed to non-cerebellum structure. This is illustrated in Figure 2, and further explained in Section II. The AM-FM amplitude describes the maximum range between the intensity minima and maxima.

0-7803-6514-3/00/$10.00©2000 IEEE

Using the amplitude, we note that we clearly have: (i) translation invariance and (ii) rotation invariance. Scale invariance is also given, since scale changes should not change the amplitude values. To achieve true scale invariance with respect to the shape analysis steps following the initial amplitude segmentation steps, we simply require that the granulometric size distributions for the new, re-scaled images, must be computed using the re-scaled version of the generator element (a circle with a 3 pixel radius, see Section II).

In this research, we did not attempt to develop an accurate segmentation algorithm using a single AM-FM parameter. Instead, an approximate segmentation is computed which may be given as input to a more accurate method like an active contour method [7].

The segmentation algorithm is described in Section II. In Section III, the results are presented and analyzed. A summary of future research work on the subject is also given.

II. Method

To develop an AM-FM segmentation algorithm, we first use the Dominant Component Analysis (DCA) algorithm to obtain estimates of the AM-FM amplitude. An analysis of the algorithm can be found in [2-4], and it is thus not repeated here. Using the amplitude, the basic segmentation steps are presented below, and followed by an analysis of each step:

Step 1. Obtain initial segmentation results using the estimated pdfs for minimum-cost classification.
Step 2. Apply ***close*** operation with a circular element of $r = 12$ pixels to produce connected components.
Step 3. Remove any holes from binary segmentation image.
Step 4. Using the initial segmentation results, estimate the noisy granulometry of the estimated cerebellum.
Step 5. Using the noisy and the prediction on what the granulometry should be, estimate n, the number of openings required for removing the noise from the image.
Step 6. Using n, apply the appropriate granulometric filter to remove noisy regions.

For minimum-cost classification, we require estimates of: (i) $p(1)$ the probability that a pixel belongs to the cerebellum, (ii) $p(2)$ the probability that a pixel is not part of the cerebellum, (iii) $p(z|1)$ the conditional probability that the pixel amplitude takes on the value z given that it is part of the cerebellum, and (iv) $p(z|2)$ the conditional probability that the pixel amplitude takes on the value z given that it is not part of the cerebellum. For the estimates, we compute all the probabilities on a manually segmented image and then use the estimates on unseen MRI images. We did not perform any averaging of the probabilities. Instead, we use probabilities estimated on the closest (in space) MRI image.

Examples of all the probability density functions involved are shown in Figure 2. We note that the amplitude distribution for the cerebellum is somewhat simple. It involves a single peak, and the peak is seen to coincide with a minimum in the non-cerebellum distribution (see upper-right plot of Figure 2). This observation suggests that this range of amplitude values can be used to identify pixels associated with the cerebellum. Nevertheless, it is also clear from the upper-right plot of Figure 2 that un-weighted classification will not work since the distribution of the cerebellum values remains strictly less than the distribution of the amplitude background pixels. This is primarily due to the fact that the cerebellum pixels account for less than 15% of the total pixels. Hence, $p(1) < 0.15$, which implies that $p(2) = 1\text{-}p(1) > 0.85$. To give approximately equal importance to the cerebellum pixels, we perform minimum cost classification with $c = 5$, and classify a pixel as a cerebellum pixel if $c \cdot p(1) \cdot p(z|1) > p(1) \cdot p(z|1)$, else classify it as background.

The initial cerebellum segmentation estimate lacks the compactness of the actual cerebellum. This motivates steps 2 and 3, where isolated regions are connected by a morphological *close* operation, and then all holes are removed. Naturally, compactness is not just brought to the desired cerebellum pixels, but it is also brought to the noisy background pixels. To remove all the noisy compact regions due to the *close* operation, we will simply need to apply a morphological *open* operation with a structural element that is of the same size as the one used in the *close* operation. In general, the optimal filter is given by:

$$M = ((((((I \circ B) \circ 2B) \circ 3B) \circ 4B) \cdots) \circ nB)$$

where the value of n needs to be estimated, $\circ$ denotes the open operation, mB denotes m self-dilations with the convex generator element B. For rotational invariance, B was taken to be a circular element with a radius of 3 pixels. For estimating n, we estimate the granulometric size distributions: (i) Φ_{est} for what the actual cerebellum size distribution is expected to be, and (ii) Φ_{img} for the noisy estimate of the cerebellum size distribution (see [5, 6] for details). Using these size

distributions, we apply a two-step algorithm to estimate n. First, for $n>3$, we compute the first value of n such that: $d\Phi_{est}(n) > d\Phi_{img}(n)$. Then, if the value of n satisfies $\Phi_{img}(n) > 0.8$, we set $n = 4$. The fundamental assumption behind the algorithm is that the manually segmented cerebellum is large compared to noisy structures in the MRI segmentation estimate. Hence, the small-diameter distribution of noisy structures in the image will stay above the estimate of the actual distribution, until the spectrum due to the large diameters associated with the actual cerebellum exceeds the noise distribution. For cases where this assumption fails, we have the second step. Failure is detected by the fact that the estimated order of the morphological filter will remain more than 80% of the estimated cerebellum pixels. In this case, we use an order of 4, which is the safest noise estimate, since the close operation in step 2 of the main segmentation algorithm is of the same order.

III. Results

The four MRI images of Figure 1 were tested by using two images for training, while leaving the other two for testing. All 24 possible permutations of the ordering of the images were investigated. Two representative automated segmentation results are given in Figure 3.

The left image in Figure 3 illustrates that the cerebellum cortex can be captured with excellent accuracy by only using the AM-FM amplitude. The right image in Figure 3 shows that this is not always the case. The cerebellum cortex is characterized by unique Frequency Modulation variation that could be used to improve on such results. The non-cortex part presented some rather unique challenges. The algorithm consistently missed the outer extends while converging to the inside circular region shown in both images in Figure 3. The encouraging observation is that the outer extends that were missed, consist of very well defined edge. Hence, an active contour segmentation algorithm initialized to the automated AM-FM results, would easily be attracted to the outer extends. Another important future research direction would be to develop 3-D segmentation algorithms.

References

[1] M.S. Pattichis, "AM-FM Transforms with Applications." Ph.D. diss., The University of Texas at Austin, 1998.

[2] J.P. Havlicek, "AM-FM Image Models." Ph.D. diss., The University of Texas at Austin, 1996.

[3] A.C. Bovik, N. Gopal, T. Emmoth and A. Restrepo, "Localized measurement of emergent image frequencies by Gabor wavelets," *IEEE Trans. on Information Theory*, vol. 38, no. 2, pp. 691-712, Mar. 1992, Special Issue on Wavelet Transforms and Multiresolution Signal Analysis.

[4] A.C. Bovik, J.P. Havlicek, M.D. Desai and D.S. Harding, "Limits on Discrete Modulated Signals," *IEEE Trans. on Signal Processing*, vol. 45, no. 4, pp. 867-879, Apr. 1997.

[5] J. Serra, *Image Analysis and Mathematical Morphology, Vol. 1.* New York, Academic Press, 1982.

[6] E. R. Dougherty, *An Introduction to Morphological Image Processing*, Belingham, Washington, SPIE Optical Engineering Press, 1992.

[7] M. Kass, A. Witkin, and D. Terzopoulos, "Snakes: Active Contour Models," *Int. J. of Comp. Vision*, vol. 1, no. 4, pp. 321-331, 1987.

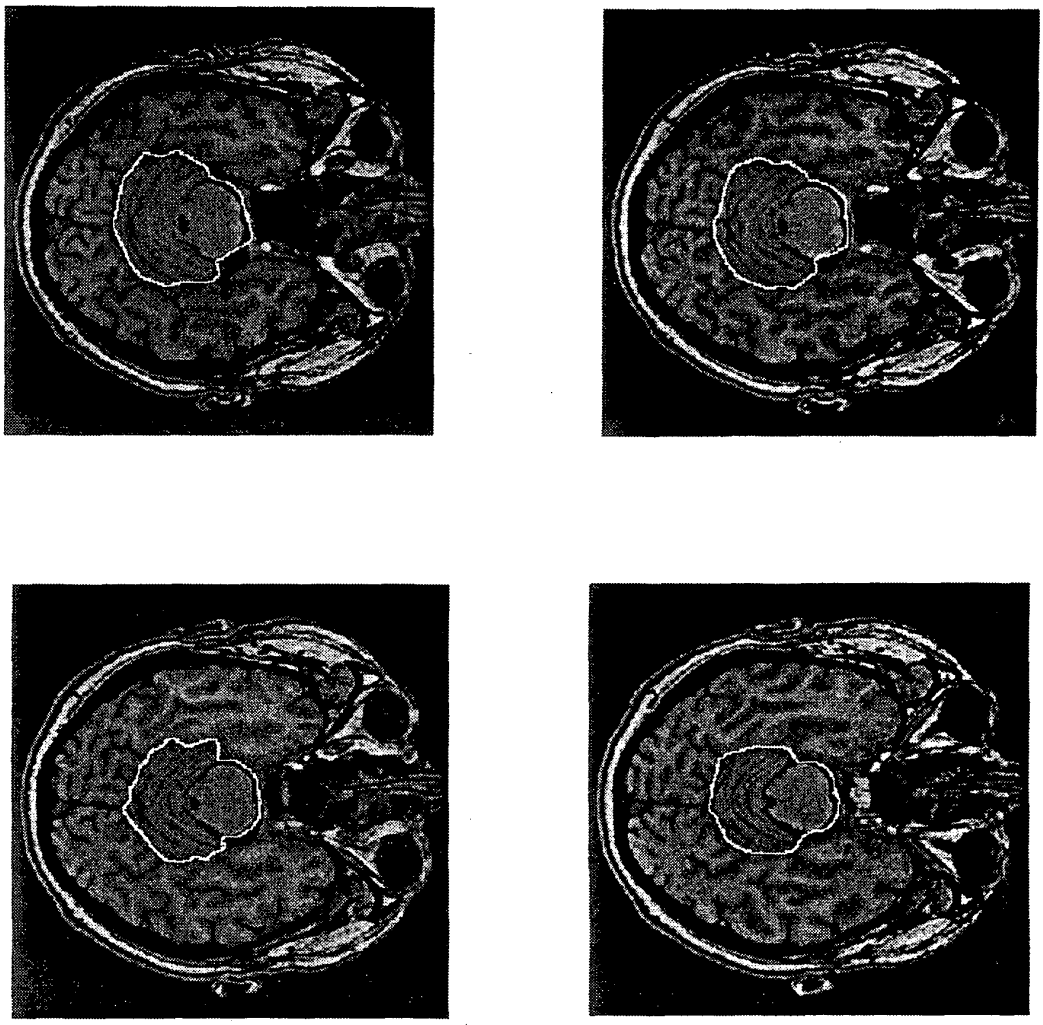

Figure 1. The manually segmented MRI images. A white line around the cerebellum denotes the boundary of the cerebellum. The images are of size 256×256.

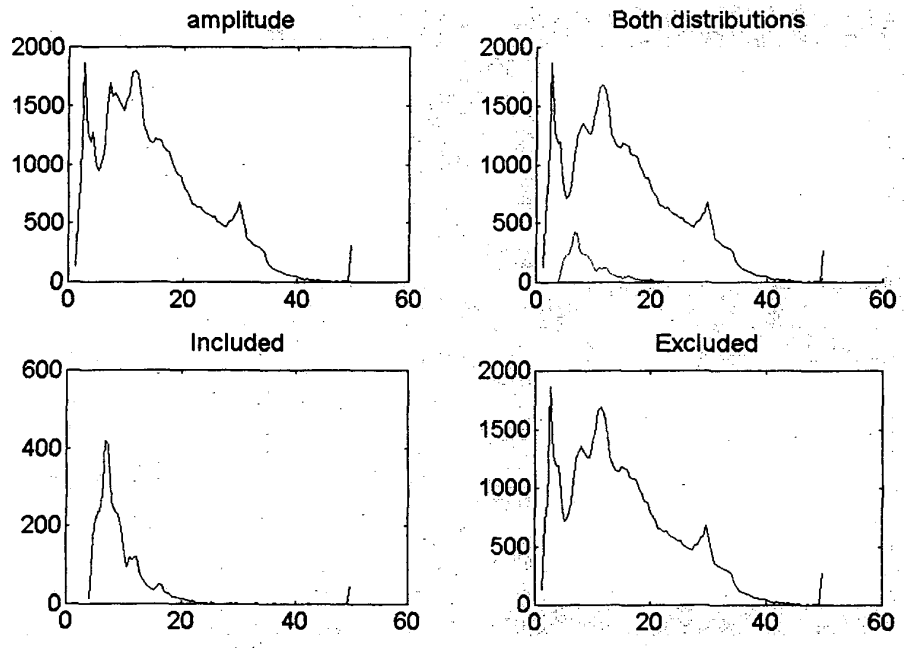

Figure 2. Amplitude histograms for the upper-left image of Figure 1. Amplitude histograms for the other MRI images share similar shapes. The upper-left plot is for the amplitude values over the entire image. The upper-right plot shows the amplitude distributions over the non-cerebellum regions (upper histogram) and the cerebellum region (lower histogram). The lower-left plot shows the histogram of the amplitude over the cerebellum. The lower-right plot shows the histogram of the amplitude over the non-cerebellum region.

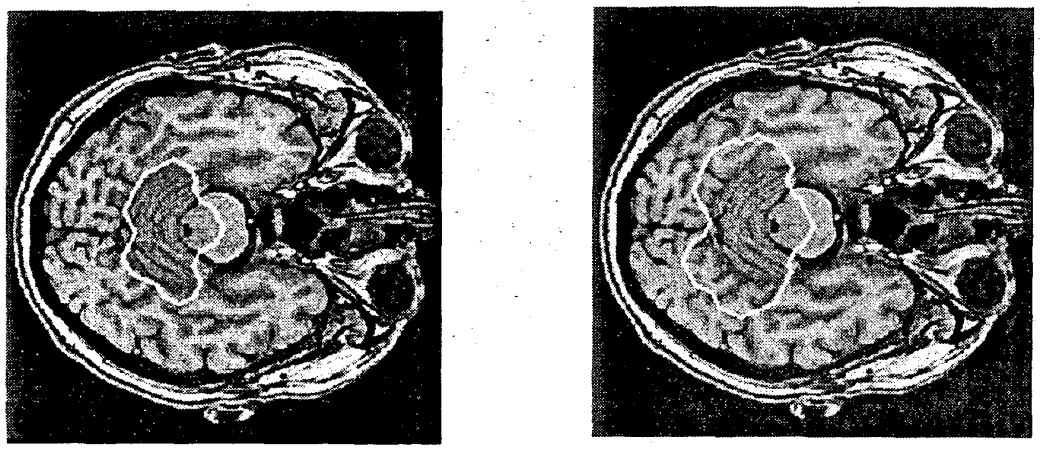

Figure 3. Automated segmentation results. For the error, we count the total number of misclassified pixels and divide by the total number of pixels in the image. The image on the left had 2.5% misclassified pixels ($n = 4$, for the granulometric filter), while the image on the right had 4.9% misclassified pixels ($n = 6$, for the granulometric filter).